Three-Dimensional Tungsten Oxide Nanowire Networks**

By *Jun Zhou*, *Yong Ding*, *Shao Z. Deng*, *Li Gong*, *Ning S. Xu*,* and *Zhong L. Wang**

Among transition metal oxides, tungsten oxides ($WO_{3-\delta}$) are of great interest and have been investigated extensively owing to their promising physical and chemical properties.[1–6] With outstanding electrochromic, optochromic, and gaschromic properties, tungsten oxides have been used to construct flat-panel displays, photoelectrochromic "smart" windows, optical modulation devices, write–read–erase optical devices, gas sensors, humidity and temperature sensors, and so forth.[1–5] Recently, some non-stoichiometric tungsten oxides have attracted considerable attention for their interesting electronic properties, especially superconductivity and charge-carrying abilities.[7]

It is well known that nanostructures have unique chemical and physical properties and can be used as elementary units of optoelectronic devices.[8–10] The synthesis of one-dimensional (1D) nanostructures and the assembly of these nanometer-scale building blocks to form ordered superstructures or complex functional architectures offer great opportunities for exploring their novel properties and for the fabrication of nanodevices.[11–13] Thus far, several techniques for the preparation of 1D tungsten oxide nanostructures have been developed.[6,14–17] Although the synthesis of tungsten oxide "microtrees" has been reported,[18] the growth of tungsten oxide nanowire networks remains challenging. In this paper we have successfully synthesized three-dimensional (3D) tungsten oxide nanowire networks using a thermal evaporation approach. Transmission electron microscopy (TEM) investigation indicates that the $WO_{3-\delta}$ nanowires have a cubic structure; this is

confirmed by X-ray diffraction results (see Supporting Information). Growth along the six equivalent ⟨100⟩ directions forms an intersectant 3D network structure. The mechanism that drives such growth is suggested to be the existence of ordered planar oxygen vacancies in the (100) and (001) planes parallel to the [010] growth direction. Field-emission characteristics of these nanowire networks have also been measured.

The tungsten oxide nanowire networks were synthesized by the thermal evaporation of W powders in the presence of oxygen. The scanning electron microscopy (SEM) images in Figure 1 show the typical morphology of the as-synthesized products. The high yield of the nanowire networks can be observed from the low-magnification SEM image in Figure 1a. The
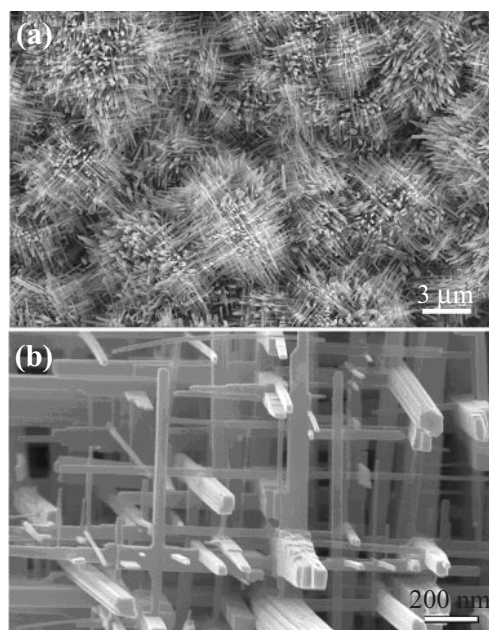

Figure 1. a) Low-magnification and b) high-magnification SEM images of the tungsten oxide nanowire networks.

high-magnification SEM image in Figure 1b clearly demonstrates the shape of the 3D nanowire network. The 3D network is constructed of nanowires with widths ranging from 10 to 180 nm. The $WO_{3-\delta}$ nanowires show a polygonal shape and intercross with each other to form the 3D network. The branches are along three perpendicular directions. Notably, there is no obvious stem in the network, making this structure different from previously reported networks and tree-like nanostructures.[11,13,18] Energy-dispersive X-ray spectroscopy (EDS) indicates the exclusive presence of W and O in the sample.

Figure 2a shows a typical TEM image of a broken $WO_{3-\delta}$ nanowire network segment with several junctions. The angle of the junctions nearly equals 90°. Selected-area electron diffraction (SAED) patterns (Figs. 2b–d) were recorded from regions B, C, and D in Figure 2a, proving that the entire network is single-crystalline; the structure could be indexed using

[*] Prof. N. S. Xu, J. Zhou, Prof. S. Z. Deng, L. Gong
State Key Lab of Optoelectronic Materials and Technologies and
Gungdong Province Key Laboratory of Display Materials and
Technologies, SunYat-Sen (Zhongshan) University
Guangzhou, 510275 (P.R. China)
E-mail: stsxns@zsu.edu.cn
Prof. Z. L. Wang, J. Zhou, Dr. Y. Ding
School of Materials Science and Engineering
Georgia Institute of Technology
Atlanta, Georgia 30332-0245 (USA)
E-mail: zhong.wang@mse.gatech.edu
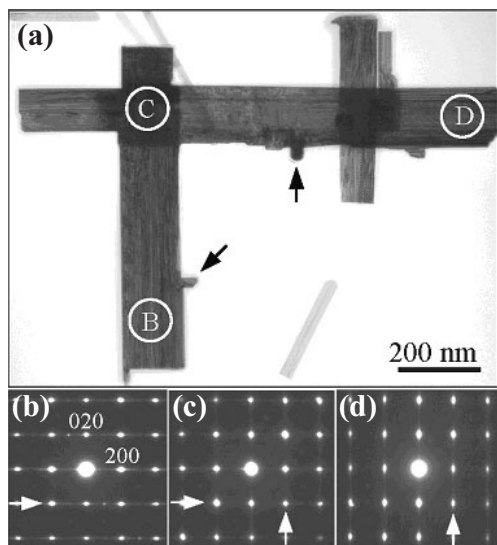
© 2005 WILEY-VCH Verlag GmbH & Co. KGaA, Weinheim **2107**

Figure 2. a) TEM image of a $WO_{3-\delta}$ nanowire network segment. b–d) SAED patterns of regions B, C, and D in (a), indicating that the network is single-crystalline. Streaks in the SAED patterns are marked by white arrowheads.
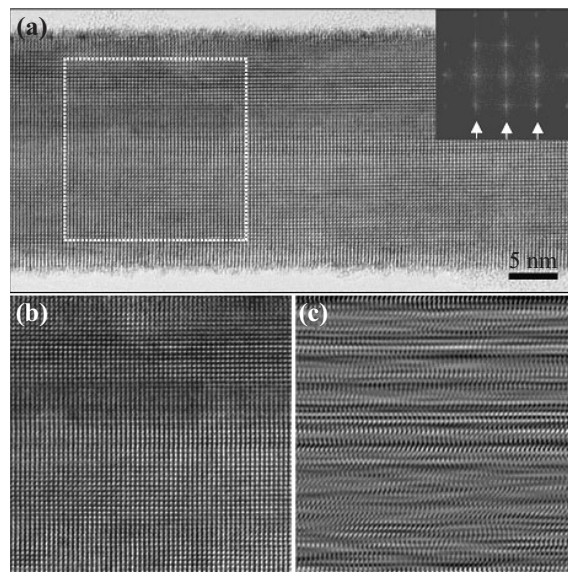

Figure 3. a) HRTEM image; inset: a FFT pattern is calculated from the square-enclosed area. b) Enlarged HRTEM image from the square-enclosed area in (a). c) Fourier-filtered image of Fig. 3b, indicating that the streaks originate from planar defects parallel to the growth direction.

body-centered cubic (bcc) WO_3.[19] The growth direction for each nanowire is along $\langle 100 \rangle$. It seems that the WO_3 nanowires grow along six equivalent $\langle 100 \rangle$ directions and then intersect with each other to form the 3D networks.

It is noticeable that there are streaks in the SAED patterns that are normal to the growth direction of the nanowires, as indicated by the white arrowheads in Figures 2b–d. These streaks in the diffraction patterns can arise from two possible causes: one is the effect of the sharp, edged shape of the nanowire, and the other is the presence of planar defects parallel to the growth direction, as seen in the TEM image in Figure 3a. High-resolution transmission electron microscopy (HRTEM) images in Figure 3 are used to distinguish between these two possibilities. Figure 3a shows a HRTEM image of a single $WO_{3-\delta}$ nanowire. The square-enclosed area is enlarged and shown in Figure 3b and its fast Fourier transform (FFT) is an inset to Figure 3a. The streaks only appear along one direction in the FFT pattern, as marked by arrowheads, indicating that the shape effect is not the main cause of the streaks. By selecting only the streaks and the center beam, the inverse FFT of the diffractogram is displayed in Figure 3c, which clearly indicates the modulation in the interplanar distance along the vertical direction, corresponding to planar defects.

The question arises as to what kind of planar defect is present in the nanowires. It cannot be stacking faults because there is no transverse displacement of the atomic columns across the defect plane. In order to characterize the defect, HRTEM simulation was carried out using Cerius2 software. The contrast of the experimental HRTEM image in Figure 4a indicates that a planar defect exists at the center, as indicated by an arrowhead. At the lower side of the defect, the non-uniform contrast might arise from the existence of oxygen vacancies. A structural model of cubic WO_3 is depicted in Figure 4c,
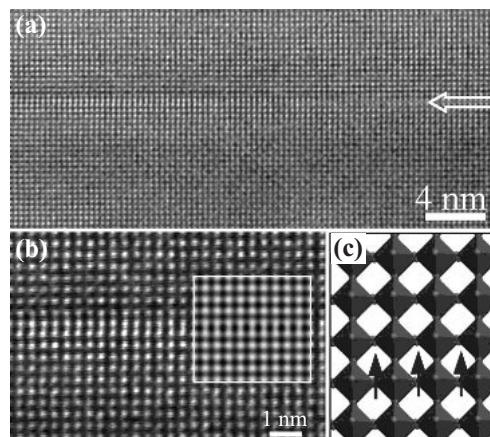
Figure 4. a) HRTEM images of a tungsten oxide nanowire with a planar defect (white arrowhead). b) Enlarged HRTEM image; inset shows a simulated image with the introduction of ordered oxygen vacancies in the (010) plane, based on the model presented in (c), where the oxygen ions that are missing are indicated by arrowheads. The simulation was for 400 kV electrons, spherical aberration coefficient, $Cs = 0.5$ mm, the objective aperture size is 8 nm^{-1}, defocus spreading is 10 nm, and beam divergence is 0.5 mrad. c) A structural model of cubic WO_3, where the oxygen ions that are missing are indicated by arrowheads.

in which the structure is constituted by the cubic packing of octahedral coordinated building blocks. Considering the oxygen vacancies that are commonly observed in tungsten oxides, we built up a planar defect model by removing oxygen atoms in the plane, as indicated by arrowheads in Figure 4c, so that the W atom is four-fold coordinated. The simulated HRTEM image (Fig. 4b, inset) fits the experimental image very well.

Owing to the cubic symmetry of the structure, these ordered and in-plane oxygen vacancies can occur equivalently in the six {100} planes. The presence of planar oxygen vacancies in the {100} planes is likely to responsible for the formation of the networks.

The synthesis process does not involve any catalyst, and thus the vapor–solid growth process may be the dominating mechanism in our case.[20] Tungsten oxide was formed by oxidizing tungsten vapor with residual oxygen in the chamber. It has been reported previously that the presence of planar defects such as stacking faults and/or the inversion grain boundaries leads to a fast growth parallel to the defect plane, forming platelet Ag nanoprisms[21] and polar-surface-dominated nanobelts,[22] respectively. For cubic structured $WO_{3-\delta}$, {100}-type low-index surfaces are likely to have the lowest energy, and thus, the nanowires are likely to be bounded by {100}-type facets. Owing to the existence of ordered in-plane oxygen vacancies in the (100) and (010) planes (see Fig. 3c), for example, fast growth of the nanowires along [001] is possible, as illustrated in Figure 5a, which is enclosed by the $\pm(100)$ and $\pm(010)$ facets. As growth proceeds, side branches enclosed by $\pm(100)$ and $\pm(001)$ facets or by $\pm(010)$ and $\pm(001)$ facets are also possibly initiated due to the creation of ordered in-plane
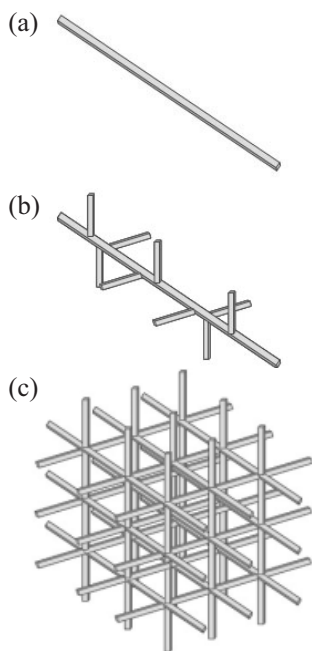
in the $\langle 100 \rangle$ family, a 3D network of interpenetrative nanowires is formed following the same process (Fig. 5c). The packs of nanowire networks in Figure 1a are likely due to multiple nucleations at the initial stage of growth.

Field-emission measurements using the transparent-anode technique were carried out in a chamber at a vacuum of $\sim 1.0 \times 10^{-7}$ torr (1 torr $= \sim 133 \times 10^2$ N m^{-2}) at room temperature.[23] Figure 6 depicts the plot of the emission current density, J, as a function of applied field, E, measured at a vacuum
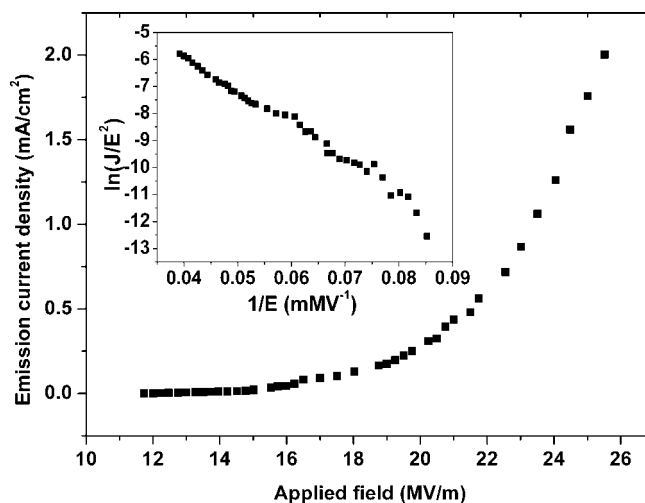

Figure 6. J–E field-emission plot of the tungsten oxide nanowire networks. Inset: the corresponding FN plot.

gap of ~ 0.2 mm. Here, we define the turn-on field as the electric field required to produce a current density of 10 μA cm^{-2}. The result shows that the tungsten oxide nanowire networks have a turn-on field of 13.85 MV m^{-1}; this value is comparable to the values reported for vertically aligned Co nanowires,[24] RuO_2 nanorods,[25] IrO_2 nanorods,[26] and ZnO nanowires.[27] The inset to Figure 6 displays the corresponding Fowler–Nordheim (FN) plot; the variation of $\ln(J/E^2)$ versus $1/E$ exhibits an approximately linear behavior, indicating that field emission from the tungsten oxide nanowire networks is a barrier-tunneling process.[28] However, at low fields, the FN plot shows deviations from linearity, which may be caused by desorption of adsorbates from the surface of the tungsten oxide nanowire networks. Since the nanowires of the 3D network point in different directions, it may be possible to design a novel field-emission nanodevice that utilizes this feature such that electron emission from the nanowires occurs in different directions. Such a device might overcome the drawback of current field-emission devices, which normally emit electrons in only one direction.

Figure 5. Schematic showing the proposed formation process for $WO_{3-\delta}$ nanowire networks. See text for details.

oxygen vacancies in the $\pm(100)$ and $\pm(001)$ planes or in the $\pm(010)$ and $\pm(001)$ planes, as is possible owing to the symmetry of the crystal structure, leading to the growth of side branches along [010] or [100], respectively (see the areas indicated by arrowheads in Fig. 2a), as illustrated in Figure 5b. Considering the six crystallographically equivalent directions

In summary, large-scale, single-crystalline cubic-structured tungsten oxide ($WO_{3-\delta}$) nanowire networks have been synthesized by the thermal evaporation of tungsten metal powder. The 3D networks are formed by interpenetrative nanowires growing along six crystallographically equivalent $\langle 100 \rangle$ direc-

tions and confined by {010} facets. It has been observed that the WO$_{3-\delta}$ nanowires are always accompanied by ordered planar defects distributed in the planes parallel to the growth direction. Combining experimental and simulated HRTEM images, we find that the planar defects are due to the accumulation of oxygen vacancies in {010} planes. The presence of ordered in-plane oxygen vacancies in the {100} planes are suggested as the driving mechanism for the formation of 3D networks. The presence of planar oxygen vacancies in (100) and (010) planes, for example, results in the growth of a nanowire along the [001] direction. 3D interpenetrative growth along the six equivalent directions of ⟨100⟩ produces the 3D network. The field-emission properties of the nanonetworks have been measured and these networks may be useful as 3D field emitters. The newly grown 3D nanowire networks could be the foundation for investigating novel applications of tungsten oxide in electrochromics, optochromics, gaschromics, and field emission.

Experimental

The tungsten oxide nanowire networks were synthesized by thermal evaporation of W powders (1 g), which were sprinkled on a W boat (120 mm × 20 mm × 0.3 mm) placed in a vacuum chamber, where the temperature, pressure, and evaporation time were controlled. The vacuum chamber was first evacuated down to about ~5 Pa. Then, high-purity argon gas (99.99 %) was introduced into the chamber. The tungsten boat was heated to ~1400–1450 °C at a heating rate of 45 °C min^{-1} and held at that temperature for 10 min, which is very important for the formation of a network structure. The chamber pressure was kept at 70 Pa (1 Pa = 1 N m^{-2}) with Ar flux at 200 standard cubic centimeters per minute (sccm). During evaporation, the tungsten oxide nanowire networks were grown on the substrates mounted above the boat, where the deposition temperature is ~950–1005 °C.

The as-synthesized products were characterized by high-resolution field-emission scanning electron microscopy (FESEM: LEO 1530 FEG at 10 kV) and transmission electron microscopy (TEM: JEOL 4000EX). The field-emission studies were carried out in a chamber having a vacuum of ~1.0 × 10^{-7} torr at room temperature. The sample area is about 4.07 mm^2, and it was first adhered to the surface of an oxygen-free high-conductivity copper disc using silver paint. A manipulator (Huntington PM-600-T) was used to control the separation (d) between the anode and the cathode. A vacuum gap (0.20 mm) was used when measuring the field-emission properties of the tungsten oxide nanowire networks. A charge-coupled device (CCD) was used to record the spatial distribution of the emission sites.

[1] C. Sanrato, M. Odziemkowski, M. Ulmann, J. Augustynski, *J. Am. Chem. Soc.* **2001**, *123*, 10639.
[2] C. G. Granqvist, *Sol. Energy Mater. Sol. Cells* **2000**, *60*, 201.
[3] S. H. Baeck, K. S. Choi, T. F. Jaramillo, G. D. Stucky, E. W. McFarland, *Adv. Mater.* **2003**, *15*, 1269.
[4] J. L. Solis, S. Saukko, L. Kish, C. G. Granqvist, V. Lantto, *Thin Solid Films* **2001**, *391*, 255.
[5] W. M. Qu, W. Wlodarski, *Sens. Actuators, B* **2000**, *64*, 42.
[6] Y. B. Li, Y. S. Bando, D. Golberg, *Adv. Mater.* **2003**, *15*, 1294.
[7] A. Shengelaya, S. Reich, Y. Tsabba, K. A. Muller, *Eur. Phys. J. B* **1998**, *12*, 13.
[8] M. H. Huang, S. Mao, H. Feick, H. Q. Yan, Y. Y. Wu, H. Kind, E. Weber, R. Russo, P. D. Yang, *Science* **2001**, *292*, 1897.
[9] C. H. Liu, J. A. Zapien, Y. Yao, X. M. Meng, C. S. Lee, S. S. Fan, Y. Lifsitz, S. T. Lee, *Adv. Mater.* **2003**, *15*, 838.
[10] W. X. Zhang, X. G. Wen, S. H. Yang, Y. Berta, Z. L. Wang, *Adv. Mater.* **2003**, *15*, 822.
[11] P. X. Gao, Z. L. Wang, *J. Phys. Chem. B* **2002**, *106*, 12653.
[12] D. L. Wang, F. Qian, C. Yang, Z. H. Zhong, C. M. Lieber, *Nano Lett.* **2004**, *4*, 871.
[13] K. A. Dick, K. Deooert, M. W. Larsson, T. Martensson, W. Seifert, L. R. Wallenberg, L. Samuelson, *Nat. Mater.* **2004**, *3*, 380.
[14] G. Gu, B. Zheng, W. Q. Han, S. Roth, J. Liu, *Nano Lett.* **2002**, *2*, 849.
[15] X. L. Li, J. F. Liu, Y. D. Li, *Inorg. Chem.* **2003**, *42*, 921.
[16] K. Lee, W. S. Seo, J. T. Park, *J. Am. Chem. Soc.* **2003**, *125*, 3408.
[17] B. C. Satishkumar, A. Govindaraj, M. Nath, C. N. Rao, *J. Mater. Chem.* **2000**, *10*, 2155.
[18] Y. Q. Zhu, W. Hu, W. K. Hsu, M. Terrones, N. Grobert, J. P. Hare, H. W. Kroto, D. R. M. Walton, H. Terrones, *Chem. Phys. Lett.* **1999**, *309*, 327.
[19] A. R. Sedle, T. E. Wood, M. L. Brostrom, D. C. Koskenmaki, B. Montez, E. Oldfield, *J. Am. Chem. Soc.* **1989**, *111*, 1665.
[20] Z. W. Pan, Z. R. Dai, Z. L. Wang, *Science* **2001**, *291*, 1947.
[21] V. Germain, J. Li, D. Ingert, Z. L. Wang, M. P. Pileni, *J. Phys. Chem. B* **2003**, *107*, 8717.
[22] Y. Ding, X. Y. Kong, Z. L. Wang, *Phys. Rev. B: Condens. Matter* **2004**, *70*, 235408.
[23] J. Zhou, N. S. Xu, S. Z. Deng, J. Chen, J. C. She, Z. L. Wang, *Adv. Mater.* **2003**, *15*, 1835.
[24] L. Vila, P. Vincent, L. D. De Pra, G. Pirio, E. Minoux, L. Gangloff, S. D. Champagne, N. Sarazin, E. Ferain, R. Lefras, L. Piraux, P. Leganeux, *Nano Lett.* **2004**, *4*, 521.
[25] C. L. Cheng, Y. F. Chen, R. S. Chen, Y. S. Huang, *Appl. Phys. Lett.* **2005**, *86*, 103104.
[26] R. S. Chen, Y. S. Huang, Y. M. Liang, C. S. Hsieh, D. S. Tsai, K. K. Tiong, *Appl. Phys. Lett.* **2004**, *84*, 1552.
[27] Y. K. Tseng, C. J. Huang, H. M. Cheng, I. N. Lin, K. S. Liu, I. C. Chen, *Adv. Funct. Mater.* **2003**, *13*, 811.
[28] R. H. Fowler, L. W. Nordheim, *Proc. R. Soc. London A* **1928**, *119*, 173.

Synthesis of PbTe Nanoboxes Using a Solvothermal Technique**

By *Wenzhong Wang,* Bed Poudel, Dezhi Wang,* and Zhi Feng Ren*

Thermoelectric (TE) materials have potential applications in electrical-energy generation, cooling, and thermal sensing. Recently, research has shown that lead chalcogenides with narrow bandgaps and face-centered-cubic structure are very promising materials for TE applications.[1–4] It has been re-

[*] Prof. Z. F. Ren, Dr. W. Z. Wang, B. Poudel, D. Z. Wang
Department of Physics, Boston College
Chestnut Hill, MA 02467 (USA)
E-mail: renzh@bc.edu; wangwm@bc.edu